Schillaci reviews the benefits and current clinical applications of scintimammography and assesses the technological developments that would allow this modality to become a routine adjunct in breast cancer imaging. . . . . ***Page 1571***

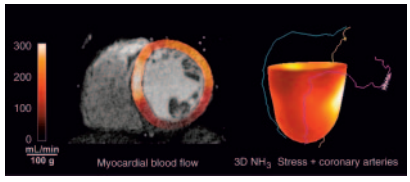

Mathieu and colleagues report on the results of a retrospective study exploring the effect of scintimammography as a complementary tool in the management of patients with inconclusive triple diagnoses (mammography, ultrasound, and fine-needle aspiration cytology) suggesting breast cancer. . . . . ***Page 1574***

Yun and colleagues compare ^{18}F-FDG PET with CT in the evaluation of primary tumors and lymph node metastases in early and advanced gastric cancer and discuss the implications of these findings for the identification of optimal initial therapies. . . . . ***Page 1582***

Elhendy and colleagues investigate whether the presence of ischemia on stress myocardial perfusion imaging is a significant predictor of deaths from all causes during long-term follow-up in patients with diabetes mellitus. . ***Page 1589***

Emmett and colleagues report on clinical factors that may influence the incidence of transient ischemic dilation on myocardial perfusion SPECT, with specific attention to the effects of left ventricular hypertrophy and diabetes. . . . . ***Page 1596***

Stankewicz and colleagues compare the effectiveness of ^{82}Rb washout studies with PET ^{18}F-FDG–^{82}Rb mismatch studies in the accurate assessment of myocardial viability in patients with coronary artery disease. . . . . ***Page 1602***

Yaoita and colleagues use myocardial perfusion scintigraphy to evaluate the regenerative effects of autologous bone marrow–derived mononuclear cell transplantation into ischemic myocardium in patients who undergo off-pump coronary artery bypass surgery. . . . . ***Page 1610***

Freedman and colleagues assess the ability of ^{11}C-L-deprenyl PET to demonstrate the specific binding characteristics of the novel irreversible selective monoamine oxidase B inhibitor rasagiline, which may have beneficial applications in the treatment of early-stage Parkinson's disease. . . . . ***Page 1618***

Drzezga and colleagues report on a longitudinal study designed to determine the combined value of genotyping and ^{18}F-FDG PET assessment of cerebral glucose metabolism in the early diagnosis of Alzheimer's type dementia in patients with mild cognitive impairment. . . ***Page 1625***

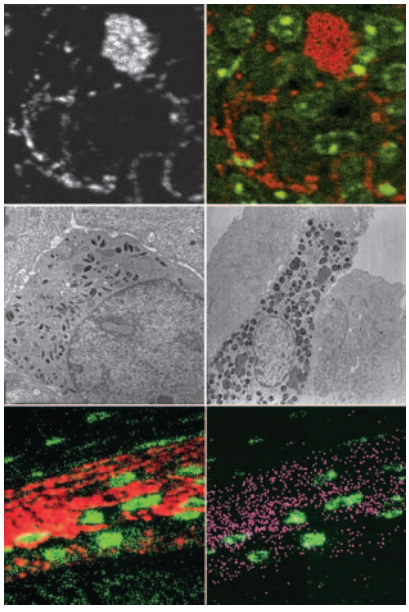

Chen and colleagues describe and validate a rapid ^{18}F-FDG PET brain imaging protocol and compare it with conventional protocols in assessing glucose metabolism in patients with and without Alzheimer's disease. . . . . ***Page 1633***

Farsad and colleagues evaluate the potential usefulness of ^{11}C-choline PET/CT for detection and localization of tumors within the prostate and compare these imaging findings with histopathologic results. . . . . ***Page 1642***

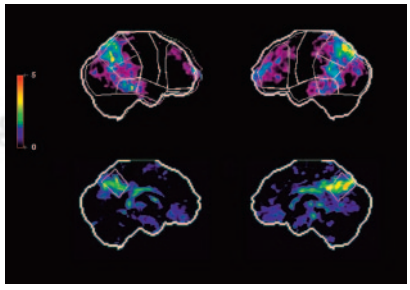

Installé and colleagues assess the ability of ^{18}F-fluoride PET to monitor therapeutic response to bisphosphonates in patients with Paget's disease and discuss the implications for routine use of whole-body PET for this purpose. . ***Page 1650***

Wong and colleagues report on a study designed to derive an optimal glucose sensitivity factor and most discriminating standardized uptake value normalized to glucose for the use of ^{18}F-FDG PET in classifying indolent and aggressive lymphomas. . ***Page 1659***

Schwaiger and colleagues review current challenges and potential for PET/CT in the routine characterization of coronary artery disease and speculate on future clinical applications in cardiology. . . . . ***Page 1664***

Jönsson and colleagues simulate scintillation camera images of patients and evaluate the accuracy of 2 methods de-

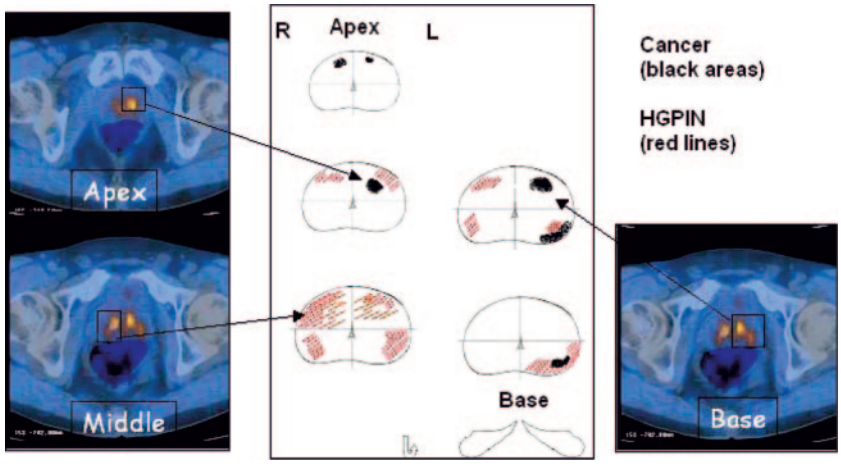

signed to minimize the confounding effects of scattered radiation from adjacent organs and activity from overlapping tissues. . . . . *Page 1679*

Lee and colleagues describe a noninvasive, fast, and accurate method for estimating myocardial blood flow and generating a parametric image using a novel linear least-squares estimation technique and $H_2^{15}O$ dynamic myocardial PET. . . . . *Page 1687*

de Jong and colleagues use ^{111}In-DTPA-octreotide SPECT in mice to investigate the role of megalin in renal tubular reabsorption of radiolabeled somatostatin analogs, with implications for tumor diagnosis and radionuclide therapy. . . . . *Page 1696*

Chéhadé and colleagues apply secondary ion mass spectrometry to obtain quantitative and qualitative data on the biodistribution of a ^{14}C-labeled melanoma-targeting molecule in mice and discuss the potential for this technique in molecular analysis of radiopharmaceutical action and distribution. . *Page 1701*

Wu and colleagues investigate a novel ^{64}Cu-labeled tetrameric RGD peptide tracer with promise for PET imaging of integrin $\alpha_v\beta_3$ expression in solid tumors and as a therapeutic radiopharmaceutical in integrin-positive tumors. . . *Page 1707*

Mathews and colleagues synthesize and evaluate in a mouse model a positron-emitting analog of a nuclear receptor that plays a central role in the control of lipid and glucose metabolism. . . . . *Page 1719*

Nock and colleagues evaluate 3 new modified ^{99m}Tc-labeled minigastrin analogs in both in vitro and animal models for their suitability in cholecystokinin subtype 2/gastrin receptor–targeted imaging of tumors. . . . . *Page 1727*

Pan and colleagues investigate a method for improving the consistency of analysis in ^{18}F-FDOPA PET images obtained to assess the diminished functionality of the striatum in patients with suspected Parkinson's disease. . . . . *Page 1737*

Chan and colleagues describe the synthesis of a novel radiolabeled recombinant vascular endothelial growth factor receptor–binding protein for imaging tumor angiogenesis. . . . . *Page 1745*

Lee and colleagues study differential glucose uptake and transport patterns in hepatocellular carcinomas and cholangiocarcinomas and discuss the potential roles of tumor-suppressor genes in these differences as well as implications for ^{18}F-FDG PET imaging of oncogenic variations. . . . . *Page 1753*

ON THE COVER

At top, nodular HCC in the inferior segment of the right lobe of the liver shows increased ^{18}F-FDG uptake on PET. Immunohistochemical staining shows a negative reaction for Glut 1 but a positive reaction for hexokinase type II (HK II). At bottom, a mass-forming cholangiocarcinoma in the inferior segment of the right lobe of the liver shows intense ^{18}F-FDG uptake. Pathologically, the tumor shows a strong positive reaction for Glut 1 along the cell membrane but a negative reaction for HK II.